NANO LETTERS

pubs.acs.org/NanoLett

Underwater Sound Generation Using Carbon Nanotube Projectors

Ali E. Aliev,* Marcio D. Lima, Shaoli Fang, and Ray H. Baughman

Alan G. MacDiarmid NanoTech Institute, University of Texas at Dallas, Richardson, Texas 75083

ABSTRACT The application of solid-state fabricated carbon nanotube sheets as thermoacoustic projectors is extended from air to underwater applications, thereby providing surprising results. While the acoustic generation efficiency of a liquid immersed nanotube sheet is profoundly degraded by nanotube wetting, the hydrophobicity of the nanotube sheets in water results in an air envelope about the nanotubes that increases pressure generation efficiency a hundred-fold over that obtained by immersion in wetting alcohols. Due to nonresonant sound generation, the emission spectrum of a liquid-immersed nanotube sheet varies smoothly over a wide frequency range, $1-10^5$ Hz. The sound projection efficiency of nanotube sheets substantially exceeds that of much heavier and thicker ferroelectric acoustic projectors in the important region below about 4 kHz, and this performance advantage increases with decreasing frequency. While increasing thickness by stacking sheets eventually degrades performance due to decreased ability to rapidly transform thermal energy to acoustic pulses, use of tandem stacking of separated nanotube sheets (that are addressed with phase delay) eliminates this problem. Encapsulating the nanotube sheet projectors in argon provided attractive performance at needed low frequencies, as well as a realized energy conversion efficiency in air of 0.2%, which can be enhanced by increasing the modulation of temperature.

KEYWORDS Carbon nanotubes, thermoacoustic, sound generation, sonar

Recent pioneering work of Fan, Jiang, and colleagues[1] has demonstrated that carbon nanotube sheets can act as powerful thermoacoustic loudspeakers, which are easy to construct and are deployable even on ordinary textiles, including a flag that is flapping in the wind. The utilized wide carbon nanotube (CNT) sheets were produced by solid-state draw from carbon nanotube forests.[2,3] The present goal is to evaluate the possibility of using this nanotube-sheet-based thermoacoustic effect for effective sound generation in liquids. The potential for high-power density, large surface area, wide-band generation of continuous, pulsed, or modulated wave output for sonar use and other in-liquid applications is of special interest. Underwater thermoacoustic generation of sound is distinctly different from conventional underwater transduction, where the physical displacement of an actuating element is required.

Thermoacoustic sound generation results from temperature variation in a carbon nanotube sheet that is produced by heating the sheet using an applied alternating voltage.[1] A hot CNT sheet heats up surrounding air in the loud speaker application, thereby inducing volume expansion and subsequent pressure waves. Due to the extremely low heat capacitance of the CNT sheet and correspondingly low thermal inertia (low density, ~1.5 mg/cm^3, and low areal density, ~3 μg/cm^2),[2] the sheet temperature synchronizes with electrical current in a wide frequency range, $1-10^5$ Hz. No mechanical vibration of a carbon multiwalled nanotube (MWNT) sheet was observed using a laser vibrometer.[1] However, at very low frequencies of 3-10 Hz in air (depending on sheet length and applied tension), mechanical resonance vibrations induced by charge injection and resulting tube-tube repulsion were observed for a high applied electrostatic potential of >100 V.[4]

Since the thermoacoustic loudspeaker acts as a heat engine, the maximum energy conversion efficiency, according to Carnot's theorem, cannot exceed $\eta = 1 - T_c/T_h$, where T_c and T_h are the absolute temperatures of the cold and hot reservoirs, respectively. For $T_c = 295$ K and $T_h = 373$ K, the efficiency limit is 20%. Taking into account heat accumulation in the bundles and blackbody radiation from the hot nanotube surface,[5] the real conversion efficiency hardly can exceed 2%. A figure like 2.5% is typical for most devices that convert mechanical or electrical energy to acoustic energy, such as musical instrument, the human voice, and even jet aircraft engines.[6]

We presently investigate the peculiarities of thermoacoustic sound generation in liquids and analyze optimal conditions for underwater sound generation using thin self-supported or supported carbon nanotube sheets that are either aligned or highly disordered and comprise either MWNTs or single-walled nanotubes (SWNTs). There are three major components to thermoacoustic sound generation efficiency from a projector sheet: (1) the ability of the projector material to be rapidly electrically heated and then to transfer heat to surrounding medium at high rate, thereby returning to a starting temperature within the excitation cycle; (2) the working medium, which enables rapid heat transfer while minimizing effective increase in the heat capacity of the projector material, and surviving possibly extreme temperature of the projector material; and (3) possible packaging, which provides protection for the pro-

* Corresponding author, Ali.Aliev@utdallas.edu.
Received for review: 01/21/2010
Published on Web: 05/27/2010

TABLE 1. The Pressure Wave Generation Coefficient ξ and Some Thermodynamic and Acoustic Parameters of Studied Media[a],[10]

	helium	argon	air	water	methanol	ethanol
ξ, kg/J	1.15×10^{-2}	3.81×10^{-2}	2.25×10^{-2}	4.28×10^{-4}	5.94×10^{-4}	5.71×10^{-4}
D, mm^2/s	163	17.8[11]	23	0.138	0.10	0.085
l, μm	72	23.8	27	2.0	1.8	1.6
ρ_o, kg/m^3	0.1786	1.784	1.2	1022	792	789
C_p, J/(m^3 K)	927.5	928.2	1204.2	4.27×10^6	2.02×10^6	1.92×10^6
$C_{20\ \mu m}$, J/(m^2 K)	0.01855	0.01856	0.024	85.4	40.3	38.5
κ, W/(m K)	0.1513	0.01772	0.025	0.6071	0.2	0.169
v_s, m/s	1011	323	343	1484	1143	1144
z, kg/(m^2 s)	180.6	576	412	1.5×10^6	0.9×10^6	0.9×10^6

[a] $f = 10$ kHz, $T = 25$ °C, and the thickness of the undensified carbon nanotube aerogel sheet is the typically observed 20 μm.

jector material and efficient transmission of internal acoustical oscillation to external locations.

For comparison purpose, we can estimate the efficiency of sound generation in gases and in liquids with close thermodynamic parameters but different rheological properties (water, methanol, and ethanol). Sound generation in gases is directly related to the ideal gas law

$$PV = nRT \tag{1}$$

where, P, V, T, and n are the gas pressure, volume, temperature, and molar amount, respectively, and R is the ideal gas constant. In an open system the periodic rise and fall in the temperature of the source material (carbon nanotube sheet) produces a continuous stream of sound energy that directly propagates away from the source as plane waves. For a hermetically sealed chamber in which the source is encapsulated between two parallel windows, n, R, and V are held constant. Then any variation of the temperature of the gas leads to a change of the pressure inside the closed chamber.

Arnold and Crandall[7] proposed in 1917 the correct physical picture for thermophones[8,9] and derived the formula for the sound pressure produced by a thermophone operating in an open system

$$p_{rms} = \left[\frac{\sqrt{D}\rho_o}{2\sqrt{\pi}T_o}\frac{\sqrt{f}}{C_s}\right]\frac{P_{input}}{r} \tag{2}$$

in which C_s is the heat capacity per unit area of the thin sheet conductor, f is the frequency of sound, $P_{input} = I^2R$ is the input electrical power proportional to the square of applied root-mean-square (rms) current I, and resistance R of the sheet, r is the distance between the thin sheet conductor and the microphone, ρ_o, T_o, and D are the density, average temperature, and thermal diffusivity of the ambient gas, respectively, and p_{rms} is the rms sound pressure (SP). In the first approximation, the piston model used for derivation of eq 2 is applicable for liquid medium as well. Since the input power and distance are variables in eq 2, we can estimate the coefficient in brackets as the pressure generation efficiency coefficient ξ. Table 1 shows the parameters needed for calculating ξ in the studied media, as well as some other useful parameters.

In the above table, D is the thermal diffusivity, $l = (D/\pi f)^{1/2}$ is the thermal diffusion length (calculated for $f = 10$ kHz), ρ_o is the density, C_p is the volumetric heat capacity, $C_{20\mu m}$ is the areal heat capacity for 20 μm thick material layer, κ is the thermal conductivity, v_s is the speed of sound, and z is the acoustic impedance. This thermal diffusion length is the distance that heat can diffuse through a gas or liquid during the time $\tau = 1/2\pi f$.[12-14] For calculation of ξ, instead of the heat capacity of the 20 μm thick unfilled MWNT aerogel sheet, we put the heat capacity of the 20 μm thick medium (air or liquid) that enters the sheet. This approximation can be made since the heat capacity and thermal inertia are mostly determined by the impregnated gas (or liquid) rather than the minute volume of MWNTs in the aerogel sheet, and the thermal diffusion length l in the studied frequency range 1 Hz−1 MHz is much longer than the diameter of individual MWNTs (∼10 nm) or bundles (∼150 nm).

Table 1 predicts that the pressure generation efficiency of a CNT sheet directly immersed in water is ∼100× lower than for gas environments, assuming that water and nanotubes are in direct contact. Furthermore, again assuming direct liquid−nanotube contact, methanol and ethanol are predicted to have slightly higher efficiencies than water as sonar projection media.

In contrast, we below experimentally demonstrate that water has ∼100× higher pressure generation efficiency than the alcohols. We further show that this dramatic increase in sonar sound projection is due to the extremely high hydrophobicity of the carbon nanotube surface, which creates a gas envelop around the CNTs. Additionally, adding 0.1% of methanol to deionized (DI) water rapidly decreased the detected SP 10-fold, likely by providing a CNT coating with alcohol that enables nanotube wetting.

We first describe thermoacoustic evaluation of highly oriented, solid-state-fabricated sheets containing ∼10 nm diameter MWNTs that are ∼400 μm long. The sheet areal density is only ∼3 μg/cm^2, and the sheet thickness is ∼20 μm before densification and ∼50 nm after densification.[2] Measurements of sound projection efficiency in water pre-

DOI: 10.1021/nl100235n | Nano Lett. 2010, 10, 2374-–2380

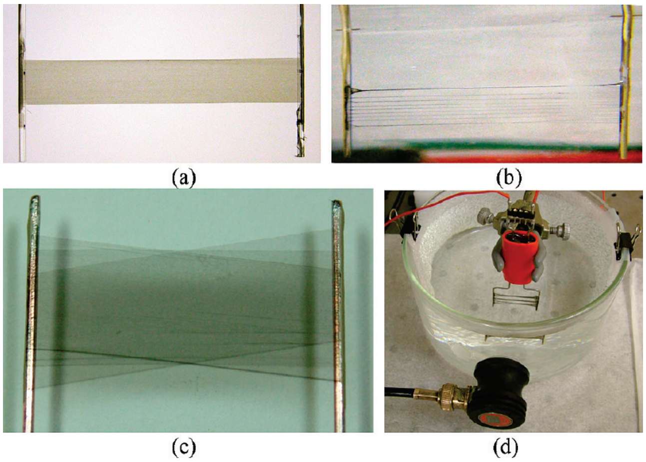

FIGURE 1. (a) A single MWNT sheet suspended between two electrodes in air. (b) A single MWNT sheet immersed in DI water has collapsed into nine very narrow strips. (c) Three stacked layers of MWNT sheets (10 × 25 mm^2) attached to two copper wires, where the nanotube orientation direction is at slightly different angles (80°, 90°, 100°) with respect to the copper wires for the different sheets, so as to provide width-direction reinforcement. (d) Experimental setup for measuring acoustic sound projection in liquids (see also Figure S1 in Supporting Information). The submersed five parallel stacked sheets split underwater into three strips.

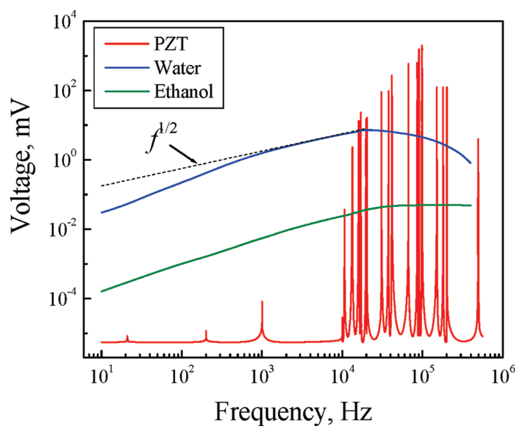

FIGURE 2. Spectra of underwater sound generation by PZT piezoceramic (red), single MWNT sheet in DI water (blue), and single MWNT sheet in ethanol (green). Spectra are normalized to the applied power and surface area of the source. The dashed line is the theoretically predicted[7] frequency dependence ($f^{1/2}$ from eq 2).

dominately used sheet stacks (suspended between two copper wires), since the high surface tension of water and the hydrophobicity of pure CNTs usually collapses a single sheet into many narrow strips (Figure 1). Sheet reinforcement was provided by this use of multilayered stacks, and by varying the orientation between the sheets in a stack to obtain a degree of lateral sheet reinforcement. The below results show that the efficiency of underwater sound generation using these sheet stacks is surprisingly high (Figure 2).

The reported SPs are expressed as the rms voltage output signal (V_{rms}) from a calibrated hydrophone having a flat frequency response (Bruel & Kjar, type 8103). These voltages are normalized to the input power per projector area. Hence, all data reported on SP can be directly compared, and correspond to relative sound generation efficiencies. Small separations between hydrophone and nanotube projector were used, where the output voltage was observed to be insensitive to this separation (since the sound waves are planar). Piezoelectric transducers having different resonant frequencies were used for both elimination of resonances, due to container dimensions, and as the main sensor for measurements at a single frequency (for the temperature and pressure dependence of nanotube projector sound pressure). These piezoelectric sensors were attached to the exterior side wall of the liquid reservoir using silicone paste (see Figure 1d), while the hydrophone was immersed in the liquid reservoir (Figure S1c,d in Supporting Information).

Figure 2 compares the SP spectra (normalized to the applied power density in W/cm^2) of a MWNT sheet and a PZT transducer (Panametrics-NDT, model V103-RB) having an especially broad emission spectra, (see Acoustic Measurements in Supporting Information). The smooth spectrum observed for the MWNT sheet between 10 Hz and 50 kHz deviates from the square root frequency dependence predicted by eq 2. This discrepancy at low frequencies between the experimental and predicted frequency dependence ($f^{1/2}$) of the sound pressure signal (SPS) is a result of the heat exchange rate between the thin film and its surrounding medium, which is omitted in the Arnold and Crandall theory.[7,1] At higher frequencies, this dependence exhibits a negative slope for all samples immersed in water. The spectrum for a multilayered MWNT sheet slightly differs from that for a single layer or a two-layer sheet stack. The negative slope onset for five stacked MWNT sheet layers starts at much lower frequencies, 8−10 kHz, which likely reflects the increasing difficulty of rapidly dissipating heat when the stack thickness increases.

While the MWNT projector provides ∼100× lower signal than the PZT at high frequencies (f ∼50−100 kHz), the former works at low frequencies much more efficiently than the PZT and does not have resonances (except those activated by the liquid container, see Supporting Information). This behavior indicates that the MWNT sheets are most suitable for SONAR application at frequencies below 4−5 kHz, with particular emphasis in the 1 kHz range where application need is high.[15] While piezoelectric actuators can also be exploited for low frequency operation, this requires very thick, heavy projectors.

To avoid collapse of a MWNT sheet during immersion into water, we attached the MWNT sheet onto a thin porous cellulose tissue (Premium grade Optical Tissue, Peca product Inc.), Figure 3. Despite possible performance degradation that could occur because of heat transfer to the supporting tissue, the sound generation efficiency increased (2×) compared with that for an unsupported MWNT sheet (which partially collapsed to form ribbons during insertion in water).

DOI: 10.1021/nl100235n | *Nano Lett.* **2010,** *10,* 2374--2380

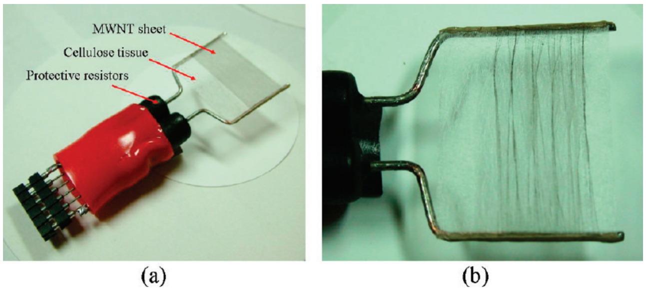

FIGURE 3. (a) MWNT sheet attached to cellulose tissue. (b) The supported MWNT sheet after five consecutive periods of underwater sound projection (each for 30 min) and subsequent drying between trial periods.

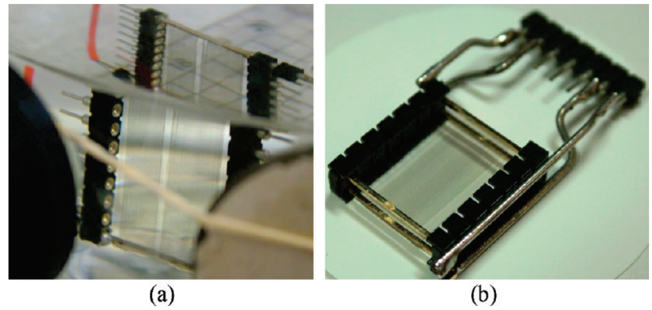

FIGURE 4. (a) Photograph of two separated MWNT sheets being dipped vertically (along the nanotube orientation direction) into methanol, showing that the sheet form is retained during the dipping process. Similar results are obtained for immersion in ethanol. The shown dual images of the sheets result from the through-glass and above-glass capture of these images. (b) Picture in air of two parallel MWNT sheets, separated by 2.5 mm perpendicular to the sheet plane, which were used for evaluation of a tandem sheet array.

The supported sheet can be used multiple times without substantial changes of sound generation efficiency.

During operation of a substrate-free MWNT sheet, the increase of average temperature, T_o, partially decreased the generated power density (see eq 2). For increasing number of sheets in the stack used for acoustic projection, heat dissipation from the stack interior by thermal conduction, convection, and blackbody radiation becomes increasingly impeded. For example, a stack of 10 MWNT sheet layers decreased sound generation efficiency by 4× with respect to that of a single sheet ($f > 1$ kHz). This degradation effect of using nanotube arrays that are too thick to provide effective heat transfer and pressure pulse release is especially seen for twisted 10 μm diameter MWNT yarns (0.8 g/cm^3), where the PZT detected signal was 1000× lower than for a single MWNT sheet immersed in water (see MWNT Yarn As a Sound Projector in the Supporting Information). Since current-generated heat was not effectively dispersed (to provide acoustic pulses), these yarns had a much lower breakdown current than for the 1 cm wide single sheet used for twist-based fabrication of the 10 μm diameter MWNT yarn.

The use of two parallel sheets spaced apart by 2.5 mm (see Figure 4b), and electrically switched alternatively using an opposite diode connection (tandem structure), eliminated the heat accumulation problem. We obtained this result by comparing the acoustical output of a two-sheet tandem structure with that for a single sheet projector (both immersed in methanol) and selecting the intersheet distance in the tandem structure to be much smaller than the acoustical wavelength but longer than the thermal diffusion length, $l < d < 0.1\lambda$. Due to the transparency of MWNT sheets to the propagating pressure waves, the cascade switching of parallel plane sources separated by a distance ΔL can enhance sound generation efficiency if the time delay between switching is close to that of sound propagation time in water, $\Delta\tau = \Delta L/4\pi v_s$. Moreover, a parallel designed transducer with properly selected spacing can work as an acoustical lens that is able to create any desired beam aperture.

MWNT sheets are readily wetted by methanol and ethanol and can be easily immersed into these liquids without producing a degraded sheet structure, as shown in Figure 4a. While the immersed MWNT sheet looks like the original flat aerogel sheet, immersion fills the sheet with alcohol that directly contacts the CNTs. This direct contact increases the thermal inertia of the acoustic source and decreases the overall efficiency. According to eq 2 the coefficient ξ in water is close to that in methanol and ethanol (see Table 1). However, the extremely high hydrophobicity of nonpolar CNT molecules to water creates air cylinders around nanotubes in sheet segments, whose diameter and gas pressure depend on surface tension and water pressure.

The experimental results show ~100× higher SPS in water than in methanol or ethanol (Figure 2). At low frequencies, the observed SP generation increases with increasing frequency, but faster than the $f^{1/2}$ of eq 2. Most important, the SP generated in water starts decreasing with increasing frequency above about 40 kHz and becomes essentially constant above 60 kHz for the ethanol sound projection medium. Perhaps, this monotonic decrease in SP signal for frequencies above $f > 40$ kHz is a result of a decrease of the diffusion length ($l = (D/\pi f)^{1/2}$, which is 13.5 μm for air at 40 kHz) to below the diameter of the air cylinders. At these higher frequencies, the SP signal decreases with increasing frequency, which is expected if the air cylinders act as a nanotube container (see below, eq 3).[7] Supporting this explanation, optical microscopy of a single MWNT sheet in water shows that the homogeneous sheet collapses into air-filled cylinders (containing nanotube sheet segments) having an average diameter of 10−20 μm.

For several samples immersed in distilled and DI water, we found the maximum of SPS to be at around 30−40 °C. Toward lower temperatures, the SPS decrease is much stronger than that at higher temperatures. The decrease of SPS toward high temperatures can be in part explained by increase of average temperature of the gas envelope, according to eq 2. However, the experimental decline is much stronger than the T^{-1} dependence of eq 2 (red dashed line in Figure 5a), so the temperature dependence of material

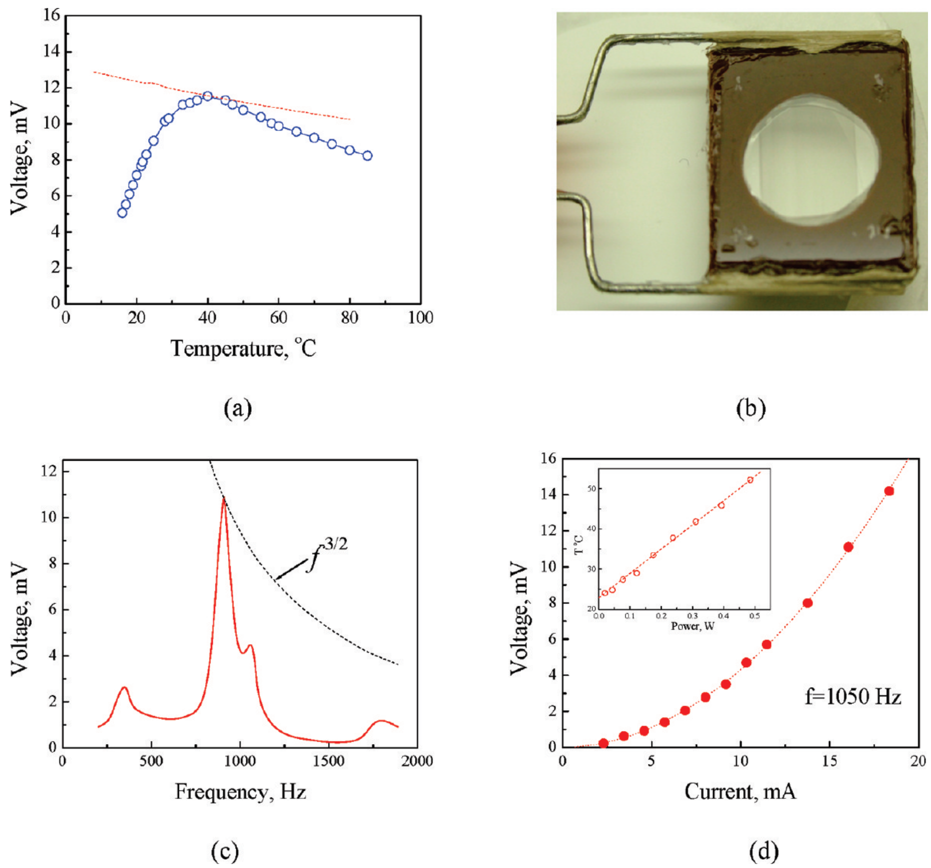

FIGURE 5. (a) The temperature dependence of SPS generated by a MWNT sheet in DI water, f = 50 kHz. The red dashed line is the T^{-1} temperature behavior of eq 2, which ignores the temperature dependences of other terms (A) in eq 2. (b) An encapsulated MWNT sheet acoustical transducer. Plastic plates (25 × 20 × 0.6 mm^3) have a central opening of 14 mm in diameter. Glass windows (0.14 mm thick) are spaced 1.2 mm apart. (c) Sound generation spectrum of an encapsulated MWNT sheet (R = 4.36 kΩ, U_o = 35 V) filled with air. The dashed line is the theoretically predicted[7] frequency dependence ($f^{3/2}$ from eq 3) for nonresonant operation. (d) The SPS versus rms ac current applied to the MWNT sheet, f_r = 1050 Hz. The inset shows the gradual evolution of the average temperature at the glass windows of an encapsulated device (measured on the external side of the window).

and structural parameters in eq 2 are likely important. Note that the maximum heat capacity of water is at 30–40 °C and the maximum water compressibility is at around 30–50 °C,[10] which is close to the observed maximum in acoustic intensity. Also, the spectral maximum (see Figure 2) is shifted with temperature to higher frequencies, from ~40 kHz (25 °C) to ~60 kHz (80 °C). The pressure dependence of SPS generated by a MWNT sheet immersed in DI water (f = 20 kHz) is flat and does not significantly depend upon hydrostatic pressure exerted by a half meter tall water cylinder.

Randomly deposited SWNT films prepared by dry-transfer technology (without exposure to surfactant or other treatment)[16] exhibit essentially the same sound generation efficiency in air as an aligned MWNT sheet and improved structural robustness when immersed into liquids. However, these SWNT sheets were wet by both water and the alcohols, so poor efficiencies were obtained (see SWNT Sheet in the Supporting Information).

Direct interaction of a CNT sheet with water is undesirable for several reasons: first, water oxidizes CNTs at high temperatures; second, high surface tension and vibration of water causes bundling of tubes into large ropes, which decreases the sound generation efficiency; third, ocean water is an ionic conductor, which can electrically short the applied voltage and cause electrochemical reactions with CNTs. To protect the MWNT sheet and avoid direct interaction of CNTs with liquid, a MWNT sheet was encapsulated in a thin flat container using various acoustically transparent windows. Figure 5b shows an acoustic transducer comprised of a MWNT sheet suspended between two plastic (phenolic cotton paper, FR-2) plates having a central circle opening (14 mm in diameter). Such openings were covered with various other window materials: glass, metallic foil, thin ceramic plate, and silicon wafer. The inner chamber was filled with air, argon, or helium. Then the edges were sealed using silicon paste. Due to resonance properties of confined space, the efficiency of low-frequency underwater sound generation significantly improved (by over 10×) compared with a nonencapsulated nanotube sheet.

The resistance of samples filled with air increased during each measurement cycle (each ~1 h long): 4.36 → 4.54 →

DOI: 10.1021/nl100235n | *Nano Lett.* **2010,** *10,* 2374--2380

4.60 kΩ. In contrast, acoustic projectors filled with inert gases (argon) showed stable acoustic projector performance for several months. Moreover, since the MWNT sheet transducer acts as a heat engine, the use of an inert-gas-encapsulated nanotube acoustic projector can enable increase of the high temperature limit for the projector to ~2000 °C, which would provide a substantially increased limiting Carnot efficiency to $\eta = 85\%$.

The production of pressure in a small enclosure is different from that for an open acoustic source.[7] In a small enclosure, where the distance between the source and walls is much smaller than the acoustic wavelength, λ, and the MWNT sheet in the nanotube orientation direction is larger than the thermal diffusion length ($l = 0.12$ mm[17] for $f = 1$ kHz), the SP produced by a thermophone is[7]

$$p_{\mathrm{rms}} = \frac{\sqrt{D}\rho_{\mathrm{o}}T_{\mathrm{s}}^{\ 1/4}}{V_{\mathrm{o}}T_{\mathrm{g}}C_{\mathrm{s}}f^{3/2}}p_{\mathrm{input}} \qquad (3)$$

where T_s is the temperature on the surface of the source (MWNT sheet), T_g is the average temperature of the filled gas, and V_o the volume of the enclosure. Note that the generated SP is predicted to decrease with increasing frequency (similar to the photoacoustic signal[12,18]), which is opposite to the open source case (see eq 2). This pressure causes the vibration of attached windows with resonance frequency: $f_r = Av_sh/a^2$, where h and a are the thickness and radius of the window and A is the coefficient of Bessel function, depending of the corresponding mode frequencies.[6] For the first resonance harmonic of a circular window with clamped edge $A_1 = 0.4694$, and for a circular plate with simply supported edge $A_1 = 0.2287$. Taking into account the "soft" attachment of the glass windows to the edges through silicon paste, one can find the resonance frequency, $f_r = 3.26$ kHz, for a simply supported (hinged) edge (v_s(glass) = 5000 m/s, $h = 0.14$ mm, $a = 7$ mm). The air encapsulated transducer shown in Figure 6 resonates at ~3.28 kHz. However, the encapsulated transducer immersed in water generates sound at much lower resonance frequencies due to the loading effect (see Figure 5c). In general, the modes of lowest frequency are decreased the most by such loading.

Substitution of the backside window with thicker glass (1 mm) increases the f_r from 908 to 1051 Hz. Window substitution on both sides with the thicker glass shifted the resonance peak toward 10 kHz, but substantially decreased acoustic intensity, in accordance with eq 3.

The detected SPS at resonance frequency is close to the square of applied current, $U_m = 0.015I + 0.042I^2$ (dashed line in Figure 5d). The deviation from quadratic behavior of generated pressure versus applied current is caused by the increase of average temperature T_g inside the enclosure and blackbody radiation from the MWNT surface, which does not contribute to SP generation. The variation of sheet resistance due to temperature change in the range of 300−600 K can be neglected. The relatively low temperature coefficient of resistivity at elevated temperatures, 10^{-4} K^{-1}, causes only ~3% resistance change in this temperature range.[19] At low applied currents, the temperature of glass window increases linearly with applied power (see inset to Figure 5d). The average temperature in the argon-filled cage was measured using an infrared temperature detector (Microtemp MT-100) on the external glass window surface, which is in air.

To estimate the energy conversion efficiency of an argon-filled encapsulated thermoacoustic transducer, we prepared several large (7.5 × 5 cm^2) devices. For a glass windows device (Figure S2 in Supporting Information) at the maximum available applied rms voltage (230 V), we obtained p_{rms} = 130 dB of SP level at 3.6 kHz in air, as measured using an impulse sound level meter (Quest Technologies, model 2700). Taking into account the electrical resistance of the encapsulated sheet (1420 Ω), we found the total electrical applied power to be $W_o = 37.5$ W. The output acoustic power for a planar acoustic source, which is independent of the distance from the plane, is approximately given by $W = 2A(p^2_{\mathrm{rms}}/\rho v_s) = 75$ mW, where A is projector area and correction is made for sound radiation in two directions. Hence, the total energy conversion efficiency of the argon encapsulated thermoacoustic transducer is $\eta = W/W_o = 0.2\%$. The flat encapsulated devices described in this study are strictly prototypes that are not designed for a specific application. There is a lot of room to increase the efficiency of encapsulated CNT sheet device (see Argon Filled Encapsulated MWNT Transducer in Supporting Information), for example, by reducing the thickness of the container (to reduce V_o in eq 3) or increasing the temperature modulation depth. The above results indicate that if the acoustic aperture of these projectors were scaled to the appropriate dimensions, they may meet the design goals of many low frequency Navy applications where thin packaging and low weight are desired. Generation of second harmonic signal by the thermoacoustic transducer is a useful feature for maintaining continuous receiver watch, instead of using frequency division multiplexing. Moreover, since the MWNT transducer is a current device, it can work at very low applied potentials (1−3 V, see Low Resistance Array in Supporting Information).

In summary, we have observed surprisingly high underwater sound generation efficiency using MWNT sheets that are self-supported or attached to porous tissue. Extremely high hydrophobicity of nonpolar CNT molecules to the highly polar water molecules enhances sound generation efficiency by creating gas cylinders around nanotube sheet segments. These structures are stable in a wide range of temperatures. Wetting of the CNT surface by methanol or ethanol decreases the SP generation efficiency ~100× (10 Hz $< f <$ 60 kHz). Adding 0.1% of methanol into DI water rapidly decreases the detected sound level ~10×. The high hydrophobicity of CNTs can be reduced by oxygen plasma treatment.[20] Plasma treatment of a solid-state-fabricated MWNT sheet (5 s exposure to a 50 W microwave plasma at 10^{-5} Torr of oxygen partial pressure) decreased SPS by a factor of 4.4 (measured in DI water in frequency range 0.1−100 kHz). Since a pure MWNT is an ideal nonpolar molecule, the detection of sound generation intensity in various media can be proposed as a very sensitive and useful tool for direct (in situ) measurement of wetting behavior of liquids and biological media. The energy conversion efficiency of flat argon encapsulated thermoacoustic transducer is found to be rather high (0.2%) and can be substantially improved by decreasing the inner volume (projector thickness) and by increasing the modulation temperature. The corresponding gravimetric capability for acoustic power projection into air, based on nanotube sheet weight, is a remarkable 0.66 kW/g, which suggests the possibility of using thin encapsulated nanotube sound projector skins for control of the boundary layer losses for air and marine vehicles.

Acknowledgment. We thank Xavier N. Lepro Chavez for preparation of plasma oxidized MWNT samples and Albert G. Nasibulin of Nanomaterials Group, Helsinki University of Technology for free-standing transparent SWNT films. This research work was supported by Office of Naval Research MURI Grant N00014-08-1-0654, Air Force Office of Scientific Research Grant FA9550-05-C-0088NSF, NSF NIRT Grant DMI-0609115, and Robert A. Welch Foundation Grant AT-0029.

Supporting Information Available. Description of acoustic measurements, argon-filled encapsulated MWNT transducer, MWNT yarn as a sound projector, and SWNT sheets having low nanotube orientation. This material is available free of charge via the Internet at http://pubs.acs.org.

REFERENCES AND NOTES

(1) Xiao, L.; Chen, Zh.; Feng, Ch.; Liu, L.; Bai, Z.-Q.; Wang, Y.; Qian, L.; Zhang, Y.; Li, Q.; Jiang, K.; Fan, Sh. *Nano Lett.* **2008**, *8* (12), 4539–4545.
(2) Zhang, M.; Fang, S. L.; Zakhidov, A. A.; Lee, S. B.; Aliev, A. E.; Williams, C. D.; Atkinson, K. R.; Baughman, R. H. *Science* **2005**, *309* (5738), 1215–1219.
(3) Liu, K.; Sun, Y. H.; Chen, L.; Feng, C.; Feng, X. F.; Jiang, K. L.; Zhao, Y. G.; Fan, S. S. *Nano Lett.* **2008**, *8* (2), 700–705.
(4) Aliev, A. E.; Oh, J.; Kozlov, M. E.; Kuznetsov, A. A.; Fang, S. L.; Fonseca, A. F.; Ovalle, R.; Lima, M. D.; Haque, M. H.; Gartstein, Y. N.; Zhang, M.; Zakhidov, A. A.; Baughman, R. H. *Science* **2009**, *323*, 1575–1578.
(5) Aliev, A. E.; Lima, M. H.; Silverman, E. M.; Baughman, R. H. *Nanotechnology* **2010**, *21*, No. 035709.
(6) Rossing, T. D.; Fletcher, N. H. *Principles of Vibration and Sound*, 2nd ed.; Springer: New York, 2004.
(7) Arnold, H. D.; Crandall, I. B. *Phys. Rev.* **1917**, *10*, 22–38.
(8) Preece, W. H. *Proc. R. Soc. London* **1879−1880**, *30*, 408–411.
(9) Braun, F. *Ann. Phys.* **1898**, *65*, 358–360.
(10) *CRC Handbook of Chemistry and Physics*, 82nd ed.; Lide, D. R., Ed.; CRC Press: New York, 2001−2002.
(11) Woodfield, P. L.; Fukai, J.; Fujii, M.; Takata, Y.; Shinzato, K. *Int. J. Thermophys.* **2008**, *29*, 1299–1320.
(12) Rosencwaig, A.; Gersho, A. *J. Appl. Phys.* **1976**, *47* (1), 64–69.
(13) Swift, G. W. *Encyclopedia of Acoustics*; Crocker, M. J., Ed.; Wiley: New York, 1997; pp 695−701.
(14) Daniel, A.; Weibull, R.; Weibull, P. *Am. J. Phys.* **2002**, *70* (12), 1231–1233.
(15) Tressler, J. F.; Howarth, T. R. *J. Electroceram.* **2002**, *8*, 175–186.
(16) Heras, A.; Colina, A.; López-Palacios, J.; Kaskela, A.; Nasibulin, A. G.; Ruiz, V.; Kauppinen, E. I. *Electrochem. Commun.* **2009**, *11* (2)), 442–445.
(17) Aliev, A. E.; Guthy, C.; Zhang, M.; Fang, S. L.; Zakhidov, A. A.; Fischer, J. E.; Baughman, R. H. *Carbon* **2007**, *45*, 2880–2888.
(18) McDonald, F. A.; Wetsel, G. C. *J. Appl. Phys.* **1978**, *49* (4), 2313–2322.
(19) Aliev, A. E.; Fridman, A. A.; Khabibullaev, P. K. *J. Commun. Technol. Electron.* **2005**, *50* (9), 1074–1081.
(20) Chirila, V.; Marginean, G.; Brandl, W. *Surf. Coatings Technol.* **2005**, *200*, 548–551.

DOI: 10.1021/nl100235n | *Nano Lett.* **2010,** *10,* 2374–-2380